The buckling resistance of welded plate girders taking into account the influence of post-welding imperfections – Part 1: Parameter study

Benjamin Launert, Cottbus, Germany, Radosław Szczerba, Marcin Gajewski, Warsaw, Poland, Michael Rhode, Berlin, Germany, Hartmut Pasternak, Cottbus, Germany and Marian Giżejowski, Warsaw, Poland

Article Information

Correspondence Address
Benjamin Launert
Brandenburgische Technische Universität (BTU) Cottbus-Senftenberg
Lehrstuhl Stahl- und Holzbau
Konrad-Wachsmann-Allee 2
Lehrgebäude 2A, Raum A.0.22
03046 Cottbus, Germany
E-mail: benjamin.launert@b-tu.de

Keywords
Welded plate girders, stability, post-welding imperfections, residual stresses, parameter study

Welding is the most important joining technique and offers the advantage of customizable plate thicknesses. On the other hand, welding causes residual stresses and deformations influencing the load carrying capacity. Their consideration in the design requires simple and fast models. Though welding simulation has contributed to accurately access to these values nowadays, their application to large components remains still in a less practicable range. Nevertheless, many studies emphasized the need to make corrections in recently available simplified models. Especially the influence of residual stresses seems somewhat overestimated in many cases if comparing conventional structural steel S355 and high-strength steel S690. In times of computer-aided design, an improved procedure to implement weld-inducted imperfections appears overdue. This will be presented in two parts. The first part illustrates the potential influence of post-welding imperfections exemplified for weak axis buckling in comparison with the general method in accordance with Eurocode 3. Residual stresses and initial crookedness were varied systematically in order to produce a scatter band of capacities. An approach to characterize the borders of these imperfections was undertaken before that. The excessive scattering of reduction factors for the load bearing capacity demonstrates the importance of these variables. Results were finally evaluated against advanced simulation models which will be further detailed in part two of this contribution.

Many standards including Eurocode 3 (EC 3) permit the use of nonlinear finite element method (FEM) calculations. The development in this field enables users to perform "experiments" in computing software instead of the laboratory or expensive in-situ experiments. Nonetheless, a sufficient implementation of all relevant input parameters remains a major task in the performance of such analysis. Compressive residual stresses and initial deformations cause strictly nonlinear component behavior. Their distribution type guides the subsequent failure and is, therefore, of crucial importance [1]. Generally, imperfections are generated by the mutual obstruction of adjacent material areas during manufacture. In terms of welding, those are due to temperature gradients and phase transformation. Depending on manufacturing parameters, boundary conditions and material properties, different more or less characteristic imperfections are created. Manufacturing parameters encompass welding parameters, but also weld sequencing or treatment measures before and after welding [2, 3]. This shows the complexity in estimation of post-welding imperfections being of interest here. This specific study refers to I-shape sections welded by conventional arc welding processes. However, similar considerations apply to other cross-sectional shapes showing the substantial need of further research in this field.

Girders are typically manufactured under workshop conditions and assembled on site.

Gas metal arc (GMAW) and submerged arc welding (SAW) are the most applied welding techniques during preproduction. They can be fully mechanized. To some extent, variation in results remains random. However, the scatter is significantly reduced in comparison with manual welding which is used on the site mainly. For this reason, it appears likely to make use of welding simulation tools made available in recent years. Industrial applications are known from mechanical engineering [4] and car manufacturing [5]. A greater application in steel construction remains uncertain though as the calculation effort and costs do not always necessarily balance the benefits of such analysis [6]. The application to large structures with several meters weld length is hardly possible today. By providing specialized software tools, the user input has been eased, but calibration and computation of the model remains expensive. The necessary discretization density around the weld and slender time stepping require immense computational effort being in the range of days even for small models [7]. Hence, the use of simplified modeling strategies remains of importance [8]. A modified procedure, suitable for the design, was presented in [9]. This will be detailed in part two of the present contribution. At first, it is important to get some idea of potential savings. Such information can be derived from numerical parameter analysis which is presented in the following.

Types and scatter of imperfections

Before moving on with the parameter study, some input parameters of this study have to be detailed. EC 3 as well as other standards distinguish so-called geometrical and structural imperfections.

Geometrical imperfections. Geometric imperfections are deviations from the ideal shape. For plated structures, the imperfections can be either global or local. Local buckling is not a particular part of this investigation, meaning that only cross sections classes 1-3 are dealt. Generally, imperfections are introduced as eigenmodes scaled to some magnitude. Typically magnitudes are defined in common with state-of-the-art manufacturing tolerances. Imperfections of the ideally straight and untwisted component may be further divided into deviations due to assembly and deviations of the member axis. The latter are referred in here. Those can be divided again into out-of-straightness (crookedness) and twist. In case of flexural failure (treated in the parameter study), the initial crookedness in each, y- and z-, direction is the relevant imperfection.

The permitted initial out-of-straightness is normally expressed as a fraction of the length of the member. EN 1090-2 defines the maximum by L/750. This value may seem rational, but it is not necessarily the right choice in the context of a probabilistic safety concept. Assuming that the statistical distributions of the initial deformations were known, it would be possible to calculate the design values to be used. However, it is not and measurements are rare. The suggested level of imperfections equal to 0.8 times the tolerance limit is based on plain engineering judgement [10]. A quite well-known magnitude used in numerical calculations is found by a thousandth of the length. The European Convention for Constructional Steelwork (ECCS) and the US Structural Stability Research Council (SSRC) used this value in the development of multiple buckling curves. The initial out-of-straightness is, on the other hand, basically a function of the manufacturing process, and some columns tend to be very straight while others do not. In favor of standardization, this was, however, necessary to limit the number of buckling curves to some reasonable amount [11]. Later, the SSRC recommended using L/1500, because this was closer to the average (L/1450) measured in laboratory columns. This value was also adopted by AISC as the governing out-of-straightness criterion.

Data for welded wide-flange shapes indicate a relatively small initial crookedness with an average of approximately L/3300 [12]. Nevertheless, reliable data are limited. Measurements presented in [13] have also shown quite small, but also variable values, though welding parameters were kept more or less similar, see also Table 1. The measurement was conducted using a photogrammetry system (TRITOP) combined with a 3D scanner (ATOS II Triple Scan). A 3D model was created and aligned in space (x is the girder axis, y- and z-axis according to Figure 2a). The out-of-straightness was defined as the deviation to a straight line connecting the end center points. The shape of the bent member is typically thought to be that of a half sine wave. The real configuration. on the other hand, can be quite complex. Modified amplitudes for the model with sinusoidal shape were recalculated. It was found that deformations are quite different with regard to the axis. Values tend to be generally higher for the deformation about the strong axis. This is expected to be due to the weld locations and the weld sequencing. However, the complexity of the bent indicates that deformations are not just due to welding. Staightness of the plates to be welded and assembly are expected to have a strong additional influence. This is particularely the case for cross sections where the positioning of welds is symmetric.

It seems, generally, rare to encounter columns with the out-of-straightness larger than the maximum permitted (and if so, those would be passed again for straightening). Nevertheless, a uniform definition throughout all types of sections is necessarily conservative. Some reference should be established for the cross-sectional shape and the manufacturing conditions. Numerical techniques (also for large structural components) have reached a level of maturity such that those can at least support this development. A principal numerical study is being processed along with part two. Nonetheless, more experiments are required.

Structural imperfections. Structural imperfections are residual stresses and variations of the yield strength across the section. The latter can have impact for hot-rolled sections, where there is some variation as a consequence of the rolling process. In welded plate girders such effect is only noticed in the heat affected zone (HAZ) and is, therefore, limited to a small area at the junction between flange and web plates. A small hardening (or for some materials possibly also softening) may be noticed. This is usually negligible in terms of

No.	1	2	3	4	5	6
y_05	0.08 (31238)	0.19 (13142)	0.63 (3959)	0.22 (11336)	0.58 (4302)	0.58 (4313)
z_05	0.13 (19223)	0.25 (9988)	1.68 (1485)	0.57 (4375)	0.89 (2803)	3.41 (733)
y_max	0.5 (4998)	0.3 (8323)	0.66 (3779)	0.29 (8600)	1.18 (2114)	1.04 (2405)
z_max	0.49 (5100)	0.47 (5313)	1.89 (1320)	0.69 (3614)	0.96 (2599)	3.64 (687)

Table 1: Measured (geometrical) imperfections, see also [13], exemplary at center position (05) compared to measured maxima (max), y indicates weak-axis deformation, z indicates strong-axis deformation, fraction of the length is indicated in brackets

load bearing capacity. The predominant influencing factors are the residual stresses. The general influence of residual stresses is to cause premature yielding. EC 3 does not propose any specific residual stress pattern. Instead, the recommendation says that a "typical" residual stress pattern should be used. This implies that values are somehow known. But usually they are not. Few more or less founded simplified distribution functions are used. However, the decision about which type of pattern fits best and is safe-sided for a particular problem is eventually on the designer.

Two quite common models used in the numerical design are shown in Figure 1. The 3D stress field is replaced by longitudinal stresses acting symmetrically on the cross section. The stresses are assumed constant throughout the thickness. The shape can be characterized by some sort of trapezoidal or block-like distribution whose borders are determined based on geometrical parameters (either dimensions [14] or plate thicknesses [15]). However, manufacturing parameters are neglected. The correlation with the material (or the yield strength in particular) is assumed to be proportional. Further, the magnitude in tension is expected to reach the yield stress of the base material. Recent studies, on the other hand, have shown this assumption to overestimate the residual stresses in many cases [16-18]. As a temporary suggestion, 500 MPa was recommended to be used as upper limit even if the actual yield strength is higher [10]. Finally, the compressive residual stresses (beeing of interest in this study) are determined from equilibrium. Therefore, their magnitude is linked with the level and extent in tension. Limitations on the applicability of the models are not reported, except for the plate thicknesses in [15] which should not exceed 40 mm. The agreement with experimental data (and corresponding simulations) was found to be more or less random in previous investigations [6, 13, 19].

Numerical welding simulation has been used to determine welding residual stresses in good agreement with experimental data [6, 13, 18, 19]. Yet, the result transfer into subsequent calculation steps remains a problem due to different demands in the simulation of welding and load bearing behavior [20]. The implementation of simulated residual stresses has shown significant deviations of the reduction factors compared with simplified residual stress models. The results indicated a large scatter in the intermediate slenderness range. This scatter band shall be detailed by the following numerical analysis. Obviously, the residual stresses in the flanges have the most significant effect on the column strength. Measured compressive residual stresses have shown amplitudes in a wide range of approximately 0.1 to a maximum of 0.5 times the yield stress. The same range was used herein.

Equivalent imperfections amplitude according to the general method (pure compression). Mostly residual stresses are still not considered explicitly. Their influence is covered along with other imperfections by so-called equivalent imperfections. The general method of EN-1993-1-1 provides the possibility of using eigenmodes. This alternative is particularly useful in complex systems if the software allows for such implementation. The scaling is recalculated based on buckling curves (e. g., European buckling curves) using linear N-M interaction:

$$e_{0,i} = \alpha \cdot \left(\sqrt{\frac{N_{pl,Rk}}{N_{cr}}} - 0.2 \right) \cdot \frac{M_{i,Rk}}{N_{pl,Rk}} \quad i = y,z \quad (1)$$

where: α is the imperfection factor for the relevant buckling curve, $N_{pl,Rk}$ is the characteristic resistance to normal force of the critical cross section, N_{cr} is the elastic critical buckling load, $M_{i,Rk}$ is the characteristic moment resistance of the critical cross section.

The use of the above mentioned method was presented in [21] in case of resistance verification of laterally restrained beam-columns. To access the global effect of imperfections, the comparison with the resistance of perfect elements is also very useful [22].

Parameter study – Buckling of columns

A parametric study on welded plate girders under uniform compression was carried out. Girders of different slenderness ratios of $\overline{\lambda}_z$ = 0.6, 0.7, 0.8, 0.9, 1.0, 1.1, 1.2, 1.3, 1.4 and cross sections as presented in Figure 2a were analyzed. The focus was on the study of the influence of geometrical and structural imperfections (namely initial crookedness and post-welding residual stresses) in case of steels S355 and S690. Cross sections are of cross section class 1 according to EN 1993-1-1. The cross-sectional area of fillet welds and welding phase transformation effects in the HAZ of the parent material are neglected. Cross section properties and plastic resistances are as follows:

S355: $A = 10\,800$ mm² (2)
$N_{pl,Rk} = 3834.0$ kN

S690: $A = 10\,800$ mm² (3)
$N_{pl,Rk} = 7452.0$ kN

The list of analyzed girders together with their slenderness ratios, corresponding lengths and Euler's critical loads ($N_{cr,z}$, $N_{cr,T}$), is given in Tables 2 and 3. A wide range of bow imperfection amplitudes was taken into account, namely from L/10000 to L/750 (where L is the length of the component). The parametric study is supplemented by calculations according to the general method (based on plastic resistance $M_{pl,Rk}$ and buck-

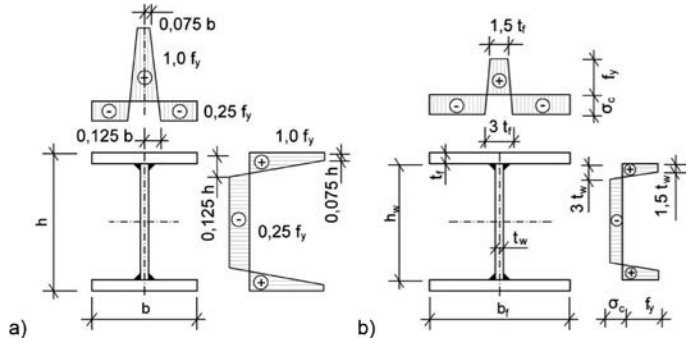

Figure 1: Simplified residual stress distributions according to a) [14] and b) [15]

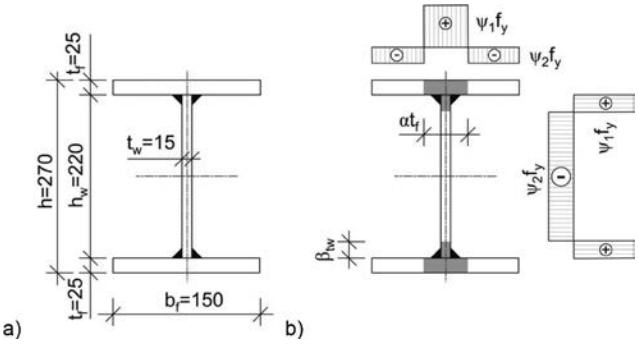

Figure 2: a) Cross section of welded plate girder, b) Distribution of post-welding residual stresses

ling curve "c") as well as verification with "perfect" geometry. In the latter case, amplitude of L/20000 was considered. The residual stresses are defined following the distribution in Figure 1. The transition area is slightly simplified and the peaks of the distribution are parametrized (see Figure 2b).

Figure 3 presents the comparison of minimal (L/10000) and maximal (L/750, tolerance limit according to EN 1090-2) bow imperfections with those determined according to the general method for buckling curve "c" with respect to slenderness ratios $\overline{\lambda}_z$. It is well visible that equivalent amplitudes based on EC 3 are much higher than those limited by EN 1090-2, but they include the influence of all imperfections, whereas in the latter case only bow imperfection amplitudes are taken into account (other imperfections must be considered separately). In case of EC 3, the relative slenderness ratio of 0.2 distinguishes the range of characteristic values of the cross section resistance and the member buckling resistance. Numerical aspects of constructing the cross section resistance interaction curves of I-sections by numerical modeling of stocky beam-columns ($\overline{\lambda}_z < 0.2$) are described in detail in [23].

The distribution of post-welding residual stresses was assumed in accordance with Figure 2b with tensile residual stresses in the vicinity of the weld and equilibrating compressive residual stresses elsewhere. For simplicity, magnitudes are assumed to be constant (also through the thickness). Tensile stresses are assumed as equal to $\psi_1 \times f_y$. For steel S355, ψ_1 is 1.0. For steel S690, $\psi_1 = 500/690$ is used according to a general recommendation in [10]. In case of compressive stresses, we assume that parameter ψ_2 is taken from the range of 0.1 to 0.5. A systematic variation in steps of 0.1 is used to illustrate their potential impact in conjunction with some initial crookedness. These values are the same in the flanges and the web in this study. Hence, widths ($\alpha \times t_f$) and ($\beta \times t_w$) are calculated based on equilibrium.

The distribution of post-welding residual stresses in the flanges is evaluated from the following equation:

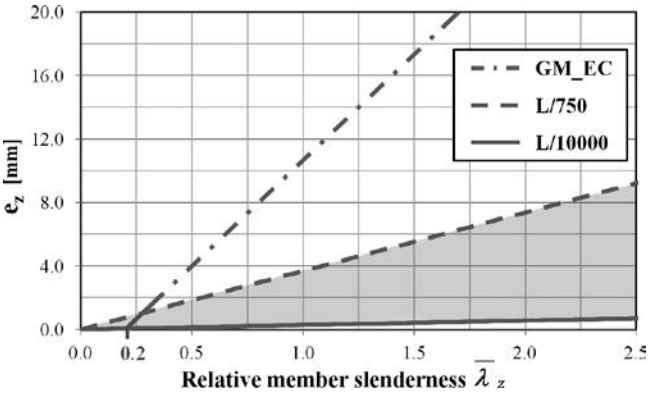

Figure 3: Values of imperfections vs. relative member slenderness, GM_EC – equivalent imperfection amplitude according to general method and buckling curve "c" of EN 1993-1-1, L/750 – maximum permitted bow amplitude according to EN 1090-2, L/10000 – minimal bow imperfection

$\overline{\lambda}_z$	L (mm)	$N_{cr,z}$ (kN)	$N_{cr,T}$ (kN)	$e_{0,z}$ GM_EC (mm) equivalent value for buckling curve formulation	$e_{1,z}$ L/20000 (mm) "perfect" element	$e_{2,z}$ L/10000 (mm)	$e_{3,z}$ L/5000 (mm)	$e_{4,z}$ L/4000 (mm)	$e_{5,z}$ L/3000 (mm)	$e_{6,z}$ L/2000 (mm)	$e_{7,z}$ L/1000 (mm)	$e_{8,z}$ L/750 (mm)
0.6	1657.9	10650.0	23576.0	5.329	0.083	0.166	0.332	0.414	0.553	0.829	1.658	2.211
0.7	1934.3	7824.5	20313.8	6.661	0.097	0.193	0.387	0.484	0.645	0.967	1.934	2.579
0.8	2210.6	5990.6	18196.5	7.993	0.111	0.221	0.442	0.553	0.737	1.105	2.211	2.947
0.9	2486.9	4733.3	16744.9	9.325	0.124	0.249	0.497	0.622	0.829	1.243	2.487	3.316
1.0	2763.2	3834.0	15706.5	10.658	0.138	0.276	0.553	0.691	0.921	1.382	2.763	3.684
1.1	3039.6	3168.6	14938.3	11.990	0.152	0.304	0.608	0.760	1.013	1.520	3.040	4.053
1.2	3315.9	2662.5	14354.0	13.322	0.166	0.332	0.663	0.829	1.105	1.658	3.316	4.421
1.3	3592.2	2268.6	13899.2	14.654	0.180	0.359	0.718	0.898	1.197	1.796	3.592	4.790
1.4	3868.5	1956.1	13538.4	15.986	0.193	0.387	0.774	0.967	1.290	1.934	3.869	5.158

Table 2: Input data for parameter analysis in case of steel S 355

$\overline{\lambda}_z$	L (mm)	$N_{cr,z}$ (kN)	$N_{cr,T}$ (kN)	$e_{0,z}$ GM_EC (mm) equivalent value for buckling curve formulation	$e_{1,z}$ L/20000 (mm) "perfect" element	$e_{2,z}$ L/10000 (mm)	$e_{3,z}$ L/5000 (mm)	$e_{4,z}$ L/4000 (mm)	$e_{5,z}$ L/3000 (mm)	$e_{6,z}$ L/2000 (mm)	$e_{7,z}$ L/1000 (mm)	$e_{8,z}$ L/750 (mm)
0.6	1189.2	20700.0	35179.3	5.329	0.059	0.119	0.238	0.297	0.396	0.595	1.189	1.586
0.7	1387.4	15208.2	28838.7	6.661	0.069	0.139	0.277	0.347	0.462	0.694	1.387	1.850
0.8	1585.6	11643.8	24723.3	7.993	0.079	0.159	0.317	0.396	0.529	0.793	1.586	2.114
0.9	1783.8	9200.0	21901.9	9.325	0.089	0.178	0.357	0.446	0.595	0.892	1.784	2.378
1.0	1982.0	7452.0	19883.7	10.658	0.099	0.198	0.396	0.496	0.661	0.991	1.982	2.643
1.1	2180.2	6158.7	18390.5	11.990	0.109	0.218	0.436	0.545	0.727	1.090	2.180	2.907
1.2	2378.4	5175.0	17254.8	13.322	0.119	0.238	0.476	0.595	0.793	1.189	2.378	3.171
1.3	2576.6	4409.5	16370.9	14.654	0.129	0.258	0.515	0.644	0.859	1.288	2.577	3.435
1.4	2774.8	3802.0	15669.6	15.986	0.139	0.277	0.555	0.694	0.925	1.387	2.775	3.700

Table 3: Input data for parameter analysis in case of steel S 690

ψ_1	ψ_2	$\alpha \times t_f$ (m m)	$\beta \times t_w$ (mm)	$\psi_1 \times f_y$ (Mpa)	$\psi_2 \times f_y$ (MPa)
1.0	**0.1**	13.6	10.0	355.0	**35. 5**
1.0	**0.2**	25.0	18.3	355.0	**71.0**
1.0	**0.3**	34.6	25.4	355.0	**106.5**
1.0	**0.4**	42.9	31.4	355.0	**142.0**
1.0	**0.5**	50.0	36.7	355.0	**177.5**

Table 4: Distribution of post-welding residual stresses in case of steel S355

ψ_1	ψ_2	$\alpha \times t_f$ (mm)	$\beta \times t_w$ (mm)	$\psi_1 \times f_y$ (Mpa)	$\psi_2 \times f_y$ (MPa)
500/690	**0.1**	18.19	13.34	500.0	**69.0**
500/690	**0.2**	32.45	23.79	500.0	**138.0**
500/690	**0.3**	43.92	32.21	500.0	**207.0**
500/690	**0.4**	53.35	39.12	500.0	**276.0**
500/690	**0.5**	61.24	44.91	500.0	**345.0**

Table 5: Distribution of post-welding residual stresses in case of steel 690

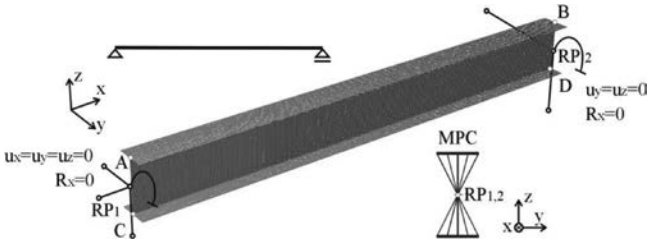

Figure 4: Numerical model with realization of boundary conditions

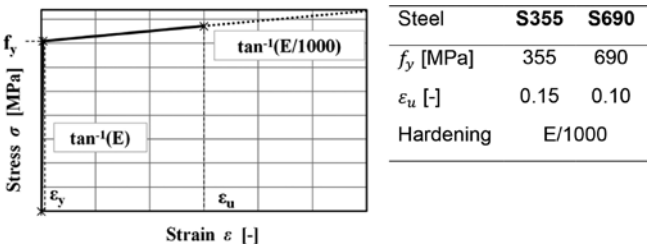

Steel	S355	S690
f_y [MPa]	355	690
ε_u [-]	0.15	0.10
Hardening	E/1000	

Figure 5: Material behavior in the uniaxial tension test of steels S355 and S690

$$\alpha \cdot t_f \cdot \psi_1 \cdot f_y \cdot t_f = (b_f - \alpha \cdot t_f) \cdot \psi_2 \cdot f_y \cdot t_f, \quad (4)$$

which finally leads to the result:

$$\alpha \cdot t_f = \frac{b_f}{\left(\frac{\psi_1}{\psi_2} + 1\right)} \quad (5)$$

Analogically, the distribution of post-welding residual stresses in the web follows due to:

$$2 \cdot \beta \cdot t_w \cdot \psi_1 \cdot f_y \cdot t_w = (h_w - 2 \cdot \beta \cdot t_w) \cdot \psi_2 \cdot f_y \cdot t_w, \quad (6)$$

which gives:

$$\beta \cdot t_w = \frac{h_w}{2 \cdot \left(\frac{\psi_1}{\psi_2} + 1\right)} \quad (7)$$

The output of Equations (5) and (7) is given in Table 4 for the flanges and in Table 5 for the web.

Residual stresses were strictly simplified in comparison to real distributions. Especially for thick plates the variation through the thickness can be quite strong locally. Neither do we have the same stresses in the flanges and the web. Nevertheless, it is known that the yielding starts from the flange tips in case of weak axis failure [6, 20]. Therefore, the influence of an advanced distribution function does not necessarily reward the expense in modeling. Accordingly, the focus of this particular study is the amplitude in compression only. Hence calculated tensile block widths (due to equilibrium) should not be mistaken.

Figure 6: Initial post-welding residual stresses (S11) in MPa in ABAQUS (S355, $\psi_2 = 0.3$)

Numerical modeling

The analyzed welded girders are simply supported ones and fully restrained to warping at both ends. Figure 4 shows the girder FEM model developed by using shell finite elements S4R (4-node element with linear shape functions and reduced integration). Calculations were carried out by ABAQUS/standard software using moderately large deformation theory (available in ABAQUS through NLGEOM option). Steels S355 and S690 were assumed to be elastic-plastic isotropic materials. In case of elasticity, the classical Hooke's relationship is assumed with Young's modulus equal to 210 GPa and Poisson ratio equal to 0.3. The plastic properties of the materials are described by plastic flow theory with Huber-Mises yield condition and isotropic strain hardening with modulus equal to E/1000. The relationship between stress and strain components in the uniaxial tension test is given in Figure 5.

The buckling resistance was assessed based on static equilibrium paths. The use of the Newton-Raphson incremental iterative algorithm (available in ABAQUS through STATIC GENERAL) with displacement control parameter allowed obtaining descending branches of the load-displacement curves so that the equilibrium paths represent both, pre- and post-limit behavior ranges. The load bearing capacity corresponds to the limit point on the path obtained for different values of bow imperfections and residual stresses. The incorporation of the residual stresses as initial stress field in ABAQUS is shown exemplary in Figure 6.

Results (FEM buckling strength of welded plate girder subjected to pure compression)

The next section presents the results of buckling strength simulations for steels S355 and S690. The list of girders and corresponding cases taken into consideration were presented in Tables 2 and 3. The distribution of post-welding residual stresses in turn is given in Tables 4 and 5.

The following abbreviations are used:

- numbers 01, 02, 03, 04, 05 indicate $\psi_2 = 0.1, 0.2, 0.3, 0.4, 0.5$,
- per_20000 – the imperfection amplitude assumed as equal to L/20000, without post-welding stresses,
- GM_EC – the imperfection amplitude according to the general method, without post-welding stresses,
- L/10000 to L/750 – considered bow imperfection amplitudes, post-welding stresses

are taken into account with respect to factors ψ_1 and ψ_2,
- solid line indicates buckling curve "c" according to EN 1993-1-1,
- gray dashed line marks Euler's hyperbola.

Figure 7 presents the static load-deformation curves in case of slenderness ratio $\overline{\lambda}_z$, factor $\psi_2 = 0.3$ for steels S355 (see Figure 7a) and S690 (see Figure 7b). Equilibrium paths corresponding to the use of the general method (only geometrical bow imperfections are taken into account) seem to be smooth in the region of critical point, whereas in cases where residual stresses are considered, characteristic peaks are well visible (extremes also occur earlier). The increase of bow imperfections amplitude generally results in "smoothing" of the equilibrium path.

Figure 8 shows deformations and equivalent stresses (v. Mises) corresponding to limit points on equilibrium paths in case of $\overline{\lambda}_z = 0.8$ for steel S355. Outcomes of the general method (GM_EC) were compared with those resulting from the application of the initial bow imperfection amplitude equal to L/1000 taking into account residual stresses with the factor $\psi_2 = 0.3$. Quite different stress distributions were noticed. Plastification always started at the inner radii of curvature. However, in case b2) PEEQ was smaller than in case a2), because the extreme on the equilibrium path occurred earlier. Also, the deformation was smaller in case b). The residual stress effect on the plastification progress was discussed, e. g., in [24].

Results of steel S355 are presented in Figures 9 to 13 in form of buckling curves, whereas the outcomes of steel S690 are shown in Figures 14 to 18. The impact of the distribution of residual stresses on the load bearing capacity is crucial for elements with relatively small slenderness ratio $\overline{\lambda}_z$. In case of slender members, the value of bow imperfection is of increasing importance and the influence of residual stresses is rather negligible. Furthermore, curves obtained for steel S690 are situated only slightly above those determined for steel S355.

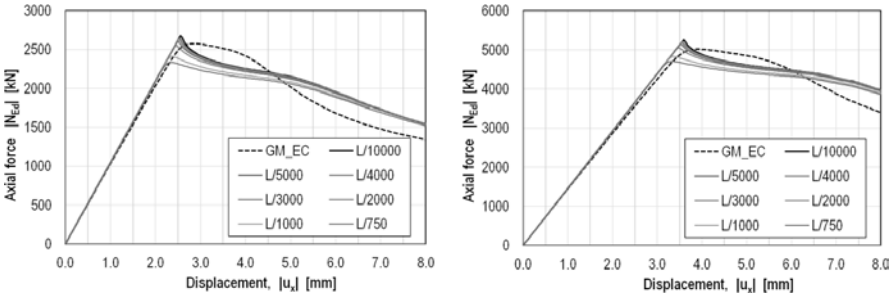

Figure 7: Static equilibrium paths in case of $\overline{\lambda}_z = 0.8$ and $\psi_2 = 0.3$ for a) S355, b) S690

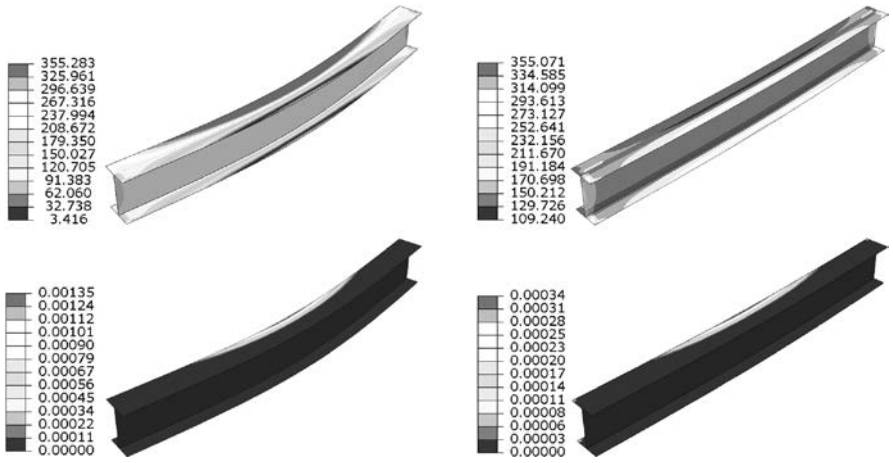

Figure 8: Equivalent stresses in MPa (1) and equivalent plastic strain (PEEQ) (2) corresponding to limit points on equilibrium paths in case of $\overline{\lambda}_z = 0.8$ and steel S355 (deformation scale factor = 10) for a) initial imperfection amplitude based on the general method and b) bow imperfection amplitude equal to L/1000 taking into account residual stresses with the factor $\psi_2 = 0.1$

Discussion

Buckling curve "c" is in good agreement with the results using the bow imperfection amplitude according to the general method in EN 1993-1-1. Calculations showed a wide scatter in load bearing capacity in case of separate definition of both, bow imperfections and residual stresses. The compliance with buckling curve "c" was best in a range of comparatively high residual stresses ($\psi_2 = 0.3$-0.4). However, the shape of the buckling curves was quite different at this stress level compared to that of the European buckling curves with some parts being both, above and below the reference line. In terms of European buckling curves, this means that this case should have been assigned by multiple curves. Regarding the bow imperfection amplitude, their particular influence in case of low slenderness is cut at higher residual stresses. This conversely means that the effect of the bow imperfection amplitude is utilized especially in case of comparatively low residual stresses.

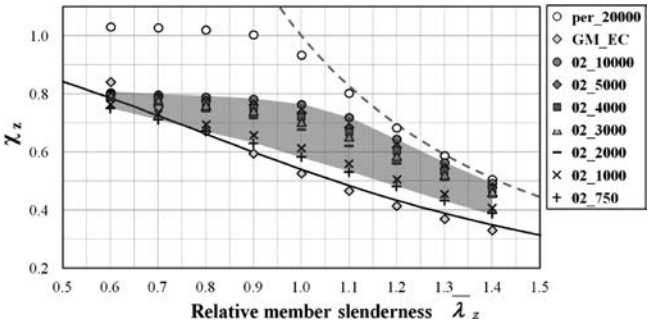

Figure 9: Results of buckling strength simulations, steel S355, $\psi_2 = 0.1$

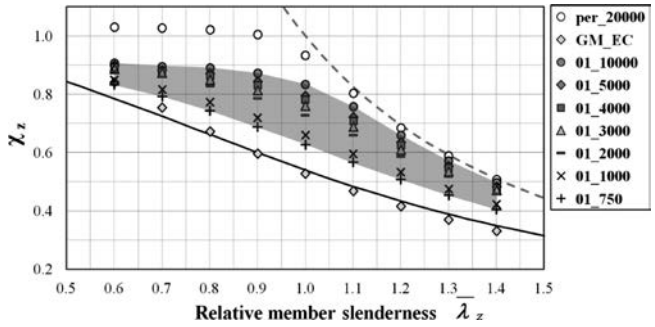

Figure 10: Results of buckling strength simulations, steel S355, $\psi_2 = 0.2$

If the reduced bow imperfection amplitude cannot be reasoned, L/1000 is still recommended as the state-of-the art manufacturing tolerance. These conditions are quite conservative, but they offer great potential for further optimization. The influence of residual stresses was significant and is illustrated again in Figure 19a for steel S355 and initial bow imperfection amplitude equal to L/1000. Values are also given for the bow imperfection amplitude equal to L/3000 for comparison in Figure 19b (this value was discussed for welded profiles at the beginning [12, 13]). The difference in load bearing capacity in the cases with $\psi_2 = 0.1$ and $\psi_2 = 0.5$ reached its maximum at $\overline{\lambda}_z = 0.9$. For lower stress levels, this maximum was shifted to lower slenderness with $\overline{\lambda}_z = 0.8$ for $\psi_2 = 0.4$ and $\overline{\lambda}_z = 0.7$ for $\psi_2 = 0.2$-0.3, respectively. Similar values apply for steel S690. The corresponding nor-

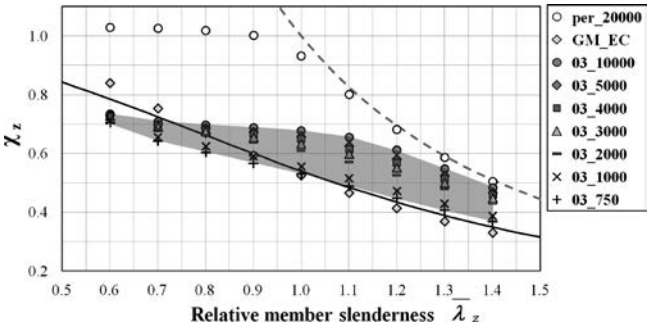

Figure 11: Results of buckling strength simulations, steel S355, $\psi_2 = 0.3$

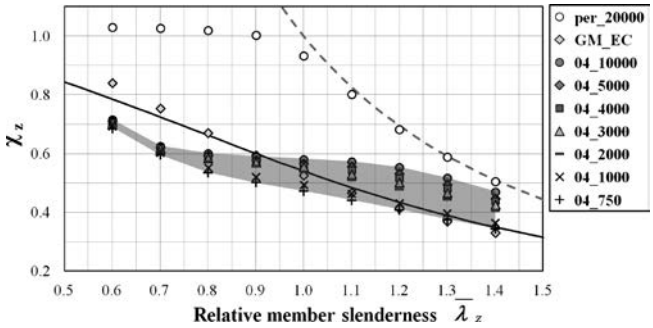

Figure 12: Results of buckling strength simulations, steel S355, $\psi_2 = 0.4$

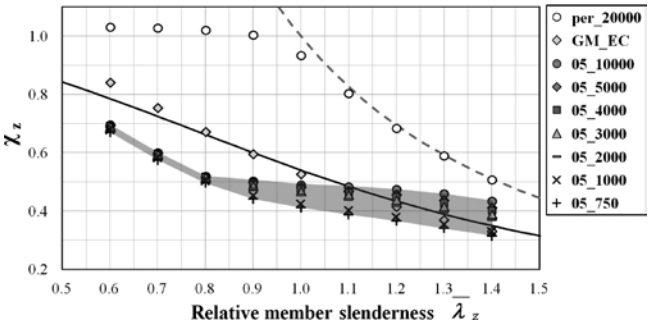

Figure 13: Results of buckling strength simulations, steel S355, $\psi_2 = 0.5$

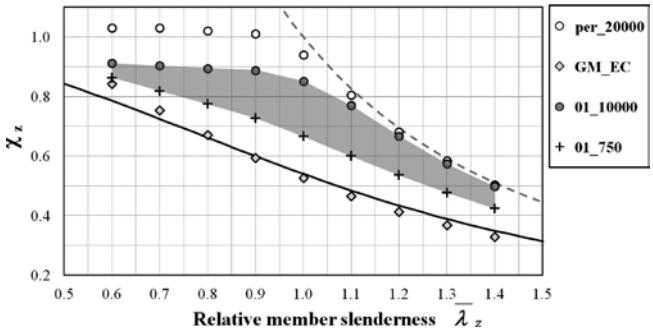

Figure 14: Results of buckling strength simulations, steel S690, $\psi_2 = 0.1$

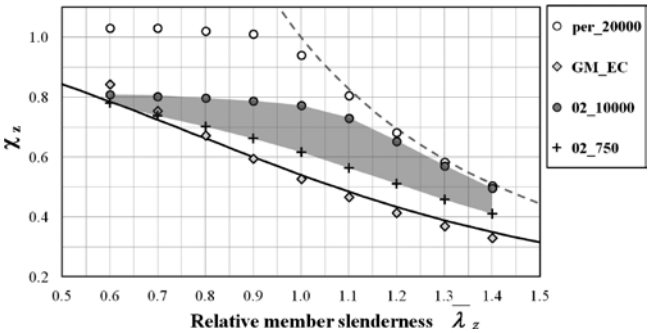

Figure 15: Results of buckling strength simulations, steel S690, $\psi_2 = 0.2$

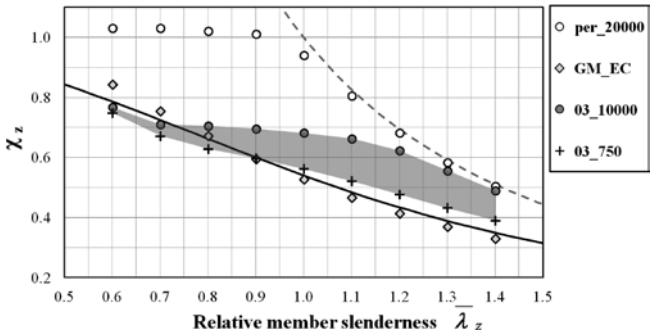

Figure 16: Results of buckling strength simulations, steel S690, $\psi_2 = 0.3$

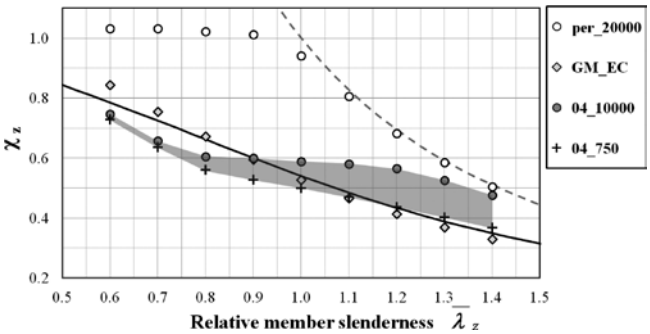

Figure 17: Results of buckling strength simulations, steel S690, $\psi_2 = 0.4$

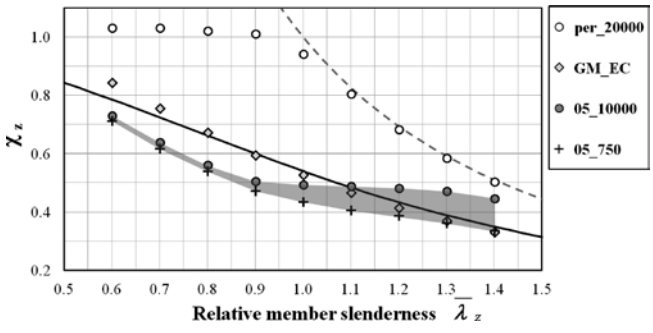

Figure 18: Results of buckling strength simulations, steel S690, $\psi_2 = 0.5$

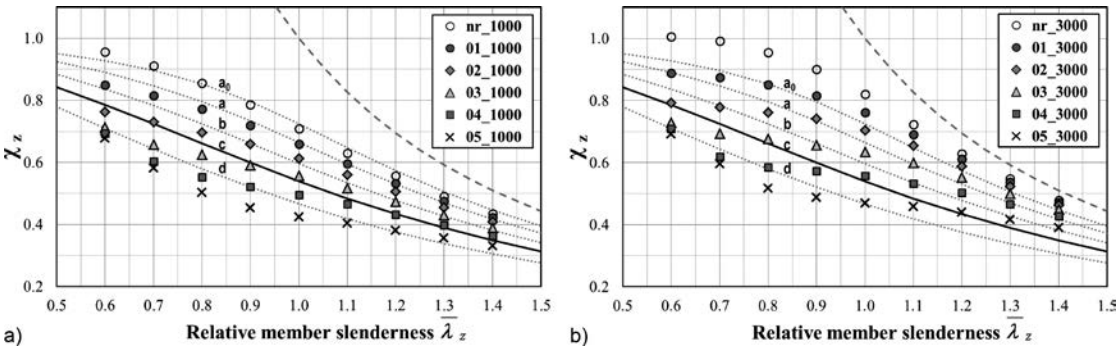

Figure 19: Influence of residual stresses (ψ_2 = 0.1-0.5), a) bow imperfection amplitude L/1000 and b) L/3000, for steel S355 (nr_1000, nr_3000 – only bow imperfection amplitude was considered)

malized values showed only minor differences (in general, values were slightly increased for S690). As a result, the assignment of a respective buckling curve could shift theoretically from curve "d" (even lower) to curve "a" and perhaps to "a_0" for some cases. This shows the recent lack in assumptions.

Real imperfections differ significantly based on geometry and manufacturing conditions but also with respect to material. For the residual stresses, it was previously found that the common assumption of a proportional increase of residual stresses with the yield strength was incorrect [13, 17-19]. This means that the buckling curve assignment in EC 3 was conservative with increasing yield strength using the same buckling curves for a wide range of constructional steels (S235 to S700). In [9], the buckling curve assignment in S690 was at least one curve higher compared to that of a respective S355 curve.

Residual stresses in steels S355 and S690. Simulations for conventional S355 and S690QL taking into account phase transformation effects (PT) were presented in [18]. Validation was based on measurements on component-like I-girders [25]. The investigated geometry is in accordance with the geometry given in Figure 2a. Material data are reported in Table 6. Welding parameters are summarized in Table 7. And residual stresses, exemplary of the flanges, are given in Figure 20. It can be generally said that normalized stresses for the S690 were approximately one half of the corresponding values of the S355.

It was also shown that numerical modeling can reproduce the residual stresses in real components. A significant transformation effect was observed only for S690. Nonetheless, this minor influenced the occurring compressive residual stresses. Generally, results showed the decreased importance of longitudinal residual welding stresses in case of S690. This implies superior buckling curve assignment. A general numerical method that directly incorporates the simulation results previously to the component design is, however, missing. This is due to dimensionality and meshing used in welding simulation on the one hand and capacity analysis on the other hand, but also due to the reduced lengths of considered components in welding simulation compared to that of built components. In a case considering phase transformation effects, differences in the applied material laws also cause problems. A practicable numerical method to account for the transfer into the component design has been presented in [9] for the first time. The model uses initial strains (based on inherent strain approach [26]) to reproduce residual stresses (and deformations) in the full-structure FE model. Residual stresses were validated. The applicability in terms of weld-induced deformations was also exemplified, but it was verified only qualitatively. Experimental backup is required.

Capacity analysis incorporating realistic residual stresses. The investigations were given for weak-axis buckling. Calculations were made by referring to denotations 1-S355 and 1-S690 in Table 7. Residual stresses were generated in a previous calculation step using initial strains. Deviations from the ideal shape were taken as the first eigenmode from linear buckling analysis (LBA) and scaled equal to L/1000. Solid element type 185 in ANSYS (Version 16.2) was used. In the case of welding, this was necessary due to the localized initial strain distribution. A 2D mesh was generated and extruded in longitudinal direction to different length (depending on slenderness). Special attention was paid to the 2D mesh generation to keep the element number small enough, but to provide also the necessary discretization density to ensure

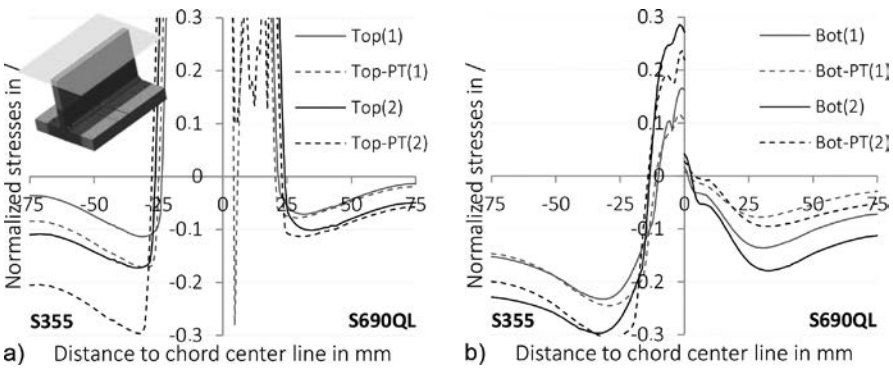

Figure 20: Normalized residual stresses of S355 and S690QL calculated by numerical welding simulation (PT-phase transformation) [18], a) top, b) bottom surface of the chords

Grade	Loc.	R_{eH} in MPa	R_m in MPa	A (%)
S355J2+N (25 mm)	Chord	**463.9**	571.8	27.9
S690QL (25 mm)	Chord	**831.3**	864.9	18.4

Table 6: Tensile test results for S355 and S690QL [18]

Girder No.	1-S355	2-S355	1-S690	2-S690
I (A)	338	327	324	329
U (V)	33.4	33.4	33.7	33.7
v (mm/s)	8.17	5.17	8.17	5.17
Q (kJ/mm)	1.39	2.11	1.34	2.14

Table 7: Welding parameters for girders 1 to 4 (geometry in accordance with Figure 2a), weld type is a single layer fillet weld, seams were welded fully-mechanized successively in PB position [18]

that initial strains are applied precisely. Works are ongoing to decrease the sensitivity of the method towards the mesh. Generally, the presented method provides a significant improvement in comparison with existent simplified models. Results of the capacity calculation were presented in [9]. A choice is given in Figure 21. The reduction factors range at the upper end of the scatter band shown in Figures 9 to 18. The comparison of the materials showed the superior buckling curve assignment for steel S690 being approximately one curve higher compared to that of steel S355.

Outlook

This present contribution outlines the importance of a suitable imperfection approach in component design. A significant scatter band in the buckling curve assignment was shown. Nowadays, the use of FEM analysis is constantly increasing, also in practice. Hence, it is a substantial matter to provide reliable rules for the future implementation of imperfections. This will help to utilize the load bearing behavior in a better way. The potential seems high, especially in case of high-strength structural steels, since imperfection amplitudes seem to be generally lower. The comparison with residual stress simulations showed that residual stresses in case of steel S690 were only half of the corresponding values in steel S355 in a case with similar welding parameters. A method was referred how to incorporate these stresses in full-structure FE models. The proposed modeling could be used to calculate geometric imperfections as well. However, the imperfection used herein may not only be welding based. Nevertheless, it can contribute to compare the weld-induced deformation in case of different material grades. Using L/1000 for all cases results in conservative assessments. This method (which can be applied for different cross sections as well) and their application scheme for the use in design will be detailed in part two. This will contribute to fill the recent gap between simulation of component manufacturing processes (in particular welding) and their implementation in the component design in advance.

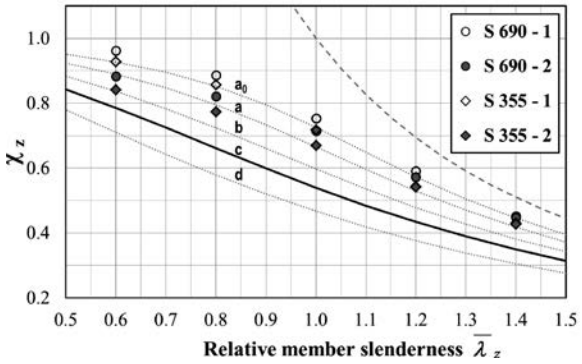

	$\bar{\lambda}_z$	1)	2)	"c"
S355	0.6	0.929	0.842	0.785
	0.8	0.857	0.774	0.662
	1.0	0.718	0.670	0.540
	1.2	0.543	0.543	0.434
	1.4	0.431	0.427	0.349
S690	0.6	0.963	0.884	
	0.8	0.886	0.822	Equal
	1.0	0.753	0.716	to
	1.2	0.592	0.572	S355
	1.4	0.452	0.447	

Figure 21: Results without (1) and with residual stresses (2) based on [9] in comparison with European buckling curves ("c"), bow imperfection amplitude was L/1000 in numerical calculations

Acknowledgement

The authors from BTU C-S and BAM thank the German Federation of Industrial Research Associations (AiF) for funding the research project IGF No. 18104 BG. This project has been carried out under the auspices of AiF and was funded by the Federal Ministry for Economic Affairs and Energy (BMWi) as part of the programme to support Industrial Community Research and Development (IGF) according to a decision of the German Bundestag.

References

1 C. Wolf: Tragfähigkeit von Stäben aus Baustahl – Nichtlineares Tragverhalten, Stabilität, Nachweisverfahren, Dissertation, Ruhr-Universität Bochum, Shaker Verlag, Aachen, Germany (2006), ISBN: 9783832252236
2 T. Kannengießer: Untersuchungen zur Entstehung schweißbedingter Spannungen und Verformungen bei variablen Einspannbedingungen im Bauteilschweißversuch, Dissertation, Otto-von-Guericke Universität Magdeburg, Shaker Verlag, Aachen, Germany (2000), ISBN: 9783826580086
3 T. Kannengießer, D. Schröpfer: Einfluss der Wärmeführung auf die Eigenspannungsausbildung und Kaltrisssicherheit in geschweißten Konstruktionen aus hochfesten Baustählen, Forschung für die Praxis, Verlag und Vertriebsgesellschaft, Düsseldorf, Germany (2015), ISBN: 9783942541572
4 D. Tikhomirov, B. Rietmann, K. Kose, M. Makkink: Computing welding distortion: Comparison of different industrially applicable methods, Advanced Materials Research 6-8 (2005), pp. 195-202 DOI:10.4028/www.scientific.net/AMR.6-8.195
5 Y. Omboko: Numerische Simulation und Kompensation von Schweißverzügen im Karosseriebau: Beitrag zur Steigerung der Maßhaltigkeit im Fertigungsprozess, Dissertation, Universität Kassel, Forschungsberichte aus der Produktionstechnik, Band 4, Shaker Verlag, Aachen, Germany (2015), ISBN: 9783844041217
6 H. Pasternak, B. Launert, T. Krausche: Welding of girder with thick plates – Fabrication, measurement and simulation, Journal of Constructional Steel Research 115 (2015), pp. 407-416 DOI:10.1016/j.jcsr.2015.08.037
7 L.-E. Lindgren: Modelling of residual stresses and deformations due to welding: "Knowing what isn't necessary to know", in: H. Cerjak, H. K. D. H. Bhadeshia (Eds.): Mathematical Modelling of Weld Phenomena 6, Maney Publishing (for The Institute of Materials, Minerals and Mining), London, UK (2002), pp. 491-518, ISBN: 9781902653563
8 C. Stapelfeld: Vereinfachte Modelle zur Schweißverzugsberechnung, Dissertation, Brandenburgische Technische Universität Cottbus-Senftenberg, Berichte des Lehrstuhls Füge- und Schweißtechnik der BTU C-S, Band 10, Shaker Verlag, Aachen, Germany (2016), ISBN: 9783844041422
9 B. Launert, M. Rhode, A. Kromm, H. Pasternak, T. Kannengießer: Residual stress influence on the flexural buckling of welded I-girders, to be published in: Materials Research Forum (2016), 10th International Conference on Residual Stresses, Sydney, Australia (2016)
10 B. Johansson, C. Müller: Annex C to EN 1993-1-5 – Finite element methods of analysis (FEM), in: B. Johansson, R. Maquoi, G. Sedlacek, C. Müller, D. Beg (Eds.): Commentary and worked examples to EN 1993-1-5 "Plated structural elements", Background documents in support to the implementation, harmonization and further development of the Eurocodes, JRC-ECCS Report No. EUR 22898 EN, 1st Edition, Luxembourg (2007), URL: http://eurocodes.jrc.ec.europa.eu/showpublication.php?id=100
11 R. D. Ziemian (Eds.): Guide to Stability Design Criteria for Metal Structures, 6th Edition, John Wiley & Sons Inc., Hoboken, New Jersey (2010), ISBN: 9780470085257
12 D. E. Chernenko, D. J. L. Kennedy: An analysis of the performance of welded wide flange columns, Canadian Journal of Civil Engineering 18 (1991), pp. 537-555 DOI:10.1139/l91-067
13 H. Pasternak, B. Launert, T. Kannengießer, M. Rhode: Residual stresses and imperfections in welded high-strength I-shape sections, in: A. Zingoni (Eds.): Insights and Innovations in Structural Engineering, Mechanics and Computation: Proceedings of the Sixth International Conference on Structural Engineering, Mechanics and Computation, Cape Town, South Africa, 5-7 September 2016, CRC Press/Balkema, Leiden, Netherlands (2016), pp. 403-404 (Hbk), pp. 1139-1146 (CD-ROM), ISBN: 9781138029279
14 N. N.: Ultimate limit state of sway frames with rigid joints, ECCS Publication No. 33, 1st Edition, Brussels, Belgium (1984)
15 N. N.: Swedish Regulations for Steel Structures – BSK 99, Boverket - Swedish National Board of Housing, Building and Planning, Karlskrona, Sweden (2003), URL: http://www.boverket.se/sv/om-boverket/publicerat-av-boverket/publikationer/2003/swedish-regulations-for-steel-structures–bsk-99/
16 M. Clarin: High Strength Steel: Local Buckling and Residual Stresses, PhD thesis, Luleå University of Technology, Sweden (2004), URL: http://epubl.ltu.se/1402-1757/2004/54/index.html
17 B. Launert, M. Rhode, H. Pasternak, T. Kannengießer: Welding residual stresses in high-strength steel - Experimental results, in:

D. Dubina, Viorel Ungureanu (Eds.): Proceedings of the International Colloquium on Stability and Ductility of Steel Structures, Timisoara, Romania, 30 May-1st June 2016, Ernst & Sohn, Berlin, Germany (2016), pp. 517-524, ISBN: 9789291471331
18 B. Launert, M.Rhode, A. Kromm, H. Pasternak, T. Kannengießer: Measurement and numerical modeling of residual stresses in welded HSLA component-like I-girders, to be published in: Welding in the World (2016), IIW-Doc. II-A-314-16, 69th IIW Annual Assembly, Melbourne, Australia (2016)
19 H. Pasternak, B. Launert, T. Kannengießer, M. Rhode: Advanced residual stress assessment of plate girders through welding simulation, to be published in: Procedia Engineering (2017), 12th International Conference Modern Building Materials, Structures and Techniques, Vilnius, Lithuania (2016)
20 T. Nitschke-Pagel, J. Klassen, H. Pasternak, B. Launert, T. Krausche: Schweißen dicker Bleche unter Baustellenbedingungen – Beurteilung des Einflusses auf das Tragverhalten von Montagestößen, Forschung für die Praxis, Verlag und Vertriebsgesellschaft, Düsseldorf, Germany (2015), ISBN: 9783942541695
21 M. Giżejowski, R. Szczerba, M. Gajewski: A unified resistance verification of beam-columns not susceptible to LT-buckling, in: M. Giżejowski et al. (Eds.): Recent Progress in Steel and Composite Structures, Proceedings of the XIII International Conference on Metal Structures, Zielona Góra, Poland, 15-17 June 2016, CRC Press/Balkema, Leiden, Netherlands, pp. 169-177, ISBN: 9781138029460 DOI:10.1201/b21417-24
22 M. Giżejowski, R. Szczerba, M. Gajewski, Z. Stachura: Beam-column resistance interaction criteria for in-plane bending and compression, Procedia Engineering 111 (2015), pp. 254-261 DOI:10.1016/j.proeng.2015.07.086
23 R. Szczerba, M. Gajewski, M. Giżejowski: Analysis of steel I-beam-columns cross section resistance with use of finite element method, Czasopismo Inżynierii Lądowej, Środowiska i Architektury (en. Journal of Civil Engineering, Environment and Architecture), z. 62 (2015), nr 3/II, pp. 425-437 DOI: 10.7862/rb.2015.166
24 M. Käsmaier, R. Ebel, M. Kraus, M. Knoblauch: Flexural buckling behavior considering different residual stress approaches, in: D. Dubina, Viorel Ungureanu (Eds.): Proceedings of the International Colloquium on Stability and Ductility of Steel Structures, Timisoara, Romania, 30 May-1st June 2016, Ernst & Sohn, Berlin, Germany (2016), pp. 501-508, ISBN: 9789291471331
25 A. Kromm, M. Rhode, B. Launert, J. Dixneit, T. Kannengießer, H. Pasternak: Combining sectioning method and X-ray diffraction for evaluation of residual stresses in welded high strength steel components, to be published in: Materials Research Forum (2016), 10th International Conference on Residual Stresses, Sydney, Australia (2016)
26 Y. Ueda, N.-X. Ma: Measuring methods of three-dimensional residual stresses with aid of distribution function of inherent strains (Report 3) – Distributions of residual stresses and inherent strains in fillet welds, Trans. JWRI 24 (1995), No. 2, pp. 123-130

Bibliography

DOI 10.3139/120.110964
Materials Testing
59 (2017) 1, pages 47-56

ISSN 0025-5300

Abstract

Zur Knicktragfähigkeit geschweißter Vollwandträger unter Berücksichtigung des Einflusses der Schweißimperfektionen – Teil 1: Parameterstudie. Schweißen gilt als die wichtigste Verbindungstechnik im Stahlbau. Es bietet den Vorteil unterschiedliche Plattendicken frei zu einem den Anforderungen entsprechenden Querschnitt zu fügen. Andererseits verursacht die Wärmewirkung beim Schweißen bleibende Spannungen und Verformung, die die Bauteiltragfähigkeit erheblich beeinflussen. Obwohl die moderne Schweißsimulation zuletzt dazu beigetragen hat, Schweißeinflüsse vergleichsweise genau vorherzusagen, ist deren Anwendung auf große Bauteile, wie sie beispielsweise im Stahlbau typisch sind, nach wie vor nicht praktikabel. Es werden somit parallel auch in Zukunft vereinfachte Berechnungsvorgehensweisen benötigt. Dennoch verdeutlicht die Schweißsimulation die Notwendigkeit verfügbare vereinfachte Berechnungsmodelle neu zu überdenken. Speziell der Eigenspannungseinfluss erscheint nach heutigem Kenntnisstand überhöht, beispielsweise im Vergleich konventioneller Baustähle wie S355 mit hochfestem Baustahl S690. In Zeiten computerorientierter Bemessungsansätze erscheint es folgerichtig, Modelle bereitzustellen, die einen konkreten Bezug zur Fertigung herstellen. Dies wird in zwei Beiträgen thematisiert. Der erste Teil des Beitrages dient dazu, den möglichen Einflussbereich der Schweißimperfektionen auf die Tragfähigkeit darzustellen. Dies erfolgt exemplarisch für das Biegeknickversagen geschweißter I-Träger um die schwache Achse im Vergleich mit der allgemeinen Bemessungsvorgehensweise nach Eurocode 3. Eingangs wird ein Versuch unternommen, geometrische und strukturelle Imperfektionen zu charakterisieren, um deren Streuweite für die Parameterstudie festzulegen. Hierin wurden Eigenspannungen und Bauteilvorkrümmung parametrisiert und systematisch variiert. Die große Streuung in den Tragfähigkeiten verdeutlicht die Wichtigkeit der Abbildung dieser Einflüsse. Die Ergebnisse werden abschließend mit erweiterten Simulationsmodellen verglichen, die in Teil 2 des Beitrages detailliert vorgestellt werden.

The authors of this contribution

M. Sc. Benjamin Launert, born in 1988, studied Civil Engineering and specialized in structural engineering at Brandenburg University of Technology (BTU) in Cottbus, Germany, from 2007 to 2012. Since 2012, he has been working as an academic assistant in the Department of Steel and Timber Structures at BTU, since 2014, he is also a PhD student in the Faculty of Architecture, Civil Engineering and Urban Development at BTU in Cottbus, Germany.

M. Sc. Radosław Szczerba, born in 1988, studied Civil Engineering at Cracow University of Technology (CUT) in Poland. From 2012 to 2015, he worked as an assistant in the Department of Building Structures at Rzeszów University of Technology (RUT), Poland. Currently, he is a PhD student in the Faculty of Civil Engineering at Warsaw University of Technology (WUT) in Poland.

Dr.-Eng. Marcin Gajewski, born in 1975, studied Civil Engineering at Warsaw University of Technology (WUT) in Poland and focused on theoretical aspects of material modeling from 1995 to 2000. In 2007, he received his PhD from the same university with the topic of constitutive and finite element modeling of isotropic and anisotropic elasto-plastic materials. He is currently working at the Department of Strength of Materials and Theory of Elasticity and Plasticity at WUT.

Dr.-Eng. Michael Rhode, born in 1983, studied Mechanical Engineering within the scope of manufacturing technologies at Otto-von-Guericke-University in Magdeburg, Germany. He finished his studies ("Dipl.-Wirtsch.-Ing.") in 2009 and received his engineering doctoral degree in 2016. Since 2011, he has been working at Bundesanstalt für Materialforschung und -prüfung (BAM) in Berlin, Germany.

Prof. Dr.-Eng. habil. Hartmut Pasternak, born in 1954, teaches steel construction at Brandenburg University of Technology (BTU) in Cottbus, Germany since 1993. He is a member of the ECCS TC8 „Structural Stability" and author (co-author) of more than 130 publications in journals and on conferences and also of 5 books. 13 doctoral students graduated under his supervision. In addition, he is a verification engineer for structures.

Prof. Dr.-Eng. habil. Marian Giżejowski, born in 1951, holds a Full Professor position at Warsaw University of Technology (WUT) in Poland. He is Chairman of the Metal Structures Division of the Civil Engineering Committee of the Polish Academy of Sciences. He worked for the University of Sydney, Australia as a postdoctoral fellow in 1983, for the University of Zimbabwe as a Senior Lecturer from 1988 to 1994 and for the University of Botswana as Associate Professor from 2001 to 2005.